frontiers in Chemistry

ORIGINAL RESEARCH
published: 24 November 2021
doi: 10.3389/fchem.2021.789249

Accurate Identification of Degraded Products of Aflatoxin B_1 Under UV Irradiation Based on UPLC-Q-TOF-MS/MS and NMR Analysis

Yan-Duo Wang[1†], Cheng-Gang Song[2†], Jian Yang[3], Tao Zhou[4], Yu-Yang Zhao[3], Jian-Chun Qin[2]*, Lan-Ping Guo[3]* and Gang Ding[1]*

[1]Key Laboratory of Bioactive Substances and Resources Utilization of Chinese Herbal Medicine, Ministry of Education, Institute of Medicinal Plant Development, Chinese Academy of Medical Sciences and Peking Union Medical College, Beijing, China, [2]College of Plant Sciences, Jilin University, Changchun, China, [3]State Key Laboratory Breeding Base of Dao-di Herbs, National Resource Center for Chinese Materia Medica, China Academy of Chinese Medical Sciences, Beijing, China, [4]Guizhou University of Traditional Chinese Medicine, Guiyang, China

Analysis, purification, and characterization of AFB_1 degraded products are vital steps for elucidation of the photocatalytic mechanism. In this report, the UPLC-Q-TOF-MS/MS technique was first coupled with purification and NMR spectral approaches to analyze and characterize degraded products of AFB_1 photocatalyzed under UV irradiation. A total of seventeen degraded products were characterized based on the UPLC-Q-TOF-MS/MS analysis, in which seven ones (1–7) including four (stereo) isomers (1,2, 5, and 6) were purified and elucidated by NMR experiments. According to the structural features of AFB_1 and degraded products (1–7), the possible photocatalytic mechanisms were suggested. Furthermore, AFB_1 and degraded products (1–7) were evaluated against different cell lines. The results indicated that the UPLC-Q-TOF-MS/MS technique combined with purification, NMR spectral experiments, and biological tests was an applicable integrated approach for analysis, characterization, and toxic evaluation of degraded products of AFB_1, which could be used to evaluate other mycotoxin degradation processes.

Keywords: aflatoxin B1, UPLC-Q-TOF-MS/MS, degraded products, purification, NMR

OPEN ACCESS

Edited by:
Wei-Lung Tseng, National Sun Yat-sen University, Taiwan

Reviewed by:
Santhana Krishna Kumar, AGH University of Science and Technology, Poland
Chi-Yu Lu, Kaohsiung Medical University, Taiwan

***Correspondence:**
Gang Ding
gding@implad.ac.cn
Lan-Ping Guo
glp01@126.com
Jian-Chun Qin
qinjc@jlu.edu.cn

†These authors have contributed equally to this work and share the first authorship

Specialty section:
This article was submitted to Analytical Chemistry, a section of the journal Frontiers in Chemistry

Received: *04 October 2021*
Accepted: *25 October 2021*
Published: *24 November 2021*

Citation:
Wang Y-D Song C-G Yang J, Zhou T, Zhao Y-Y Qin J-C Guo L-P and Ding G (2021) Accurate Identification of Degraded Products of Aflatoxin B_1 Under UV Irradiation Based on UPLC-Q-TOF-MS/MS and NMR Analysis. Front. Chem. 9:789249. doi: 10.3389/fchem.2021.789249

INTRODUCTION

Aflatoxins (AFBs), a group of mycotoxins (including AFB_1, AFB_2, $AFBG_1$, AFG_2, and other derivatives) with highly toxic, mutagenic, and carcinogenic activities, are mainly produced by *Aspergillus flavus* and *A. parasiticus* (Massey et al., 1995; Rustom, 1997). These two fungi could infect plants, grains, food, and animals which could lead to significant food safety problems and economic losses. The core skeleton of AFBs is dihydrofuro [2,3-b]furan combined with a coumarin ring, in which the double bond on the furan ring is the key toxic group. The double bond (C-8/C-9) could be transformed to AFB-8,9-epoxide in the human body, which then quickly combines with DNA, glutathione *S*-transferase, or N7 guanine to form highly toxic adducts (Garner et al., 1971; Essigmann et al., 1977; Lin et al., 1977; Croy et al., 1978).

Aflatoxin B_1 is the most notorious type with potential teratogenic, mutagenic, and hepatocarcinogenic toxicity, and it is classified as a group I carcinogen by the International Agency for Research in Cancer (IARC) (Cancer, 1993). Thus, degradation or reduction of AFB_1 becomes a hot spot worldwide. Diverse approaches including physical, chemical, and biological methods are used to degrade or reduce AFBs (Alberts et al., 2009; Mendez-Albores et al., 2009; Liu et al., 2010; Liu et al., 2011; Luo et al., 2014; Kumar et al., 2017; Peng et al., 2018). Physical methods mainly include high temperature, irradiation, adsorption, and ultrasonic methods, among which UV irradiation is often employed as an effective method to degrade or reduce AFBs based on the photosensitive characteristics (Calado et al., 2014). Liu investigated the photodegradation of AFB_1 in water/acetonitrile solution and characterized three degraded products based on UPLC-Q-TOF MS data (Liu et al., 2010). Later, they analyzed AFB_1 photodegradation in peanut oil under UV irradiation and concluded that the mutagenic effects of UV-treated samples were completely lost compared with those of untreated samples (Liu et al., 2011). Mao analyzed the degraded products of AFB_1 in peanut oil using the UPLC-Q-TOF-MS/MS technique (Mao et al., 2016). Wang investigated the degraded products using the LC-MS/MS approach and postulated toxicity of AFB_1 in methanol–water solution irradiated with Co^{60} gamma-rays (Wang et al., 2011). Recently, Li's group investigated the photodegraded inactivation mechanism of the hypertoxic site in aflatoxin B_1 by HPLC-MS (Mao et al., 2019).

Obtaining pure AFB_1-degraded products and elucidating their structures are very important to establish the photodegradation mechanism and toxic evaluation. Usually, due to limited amounts, purification of AFB_1-degraded products was significantly difficult. Thus, most mycotoxin-degraded products were mainly characterized by LC-MS/MS techniques without further separation. The LC-MS/MS technique is a high-efficient and sensitive approach for analysis and structural characterization of different metabolites in mixtures, which is often used to dereplicate or detect new compounds from extracts or characterize mycotoxin-degraded products. Yet, this technique could not differentiate (stereo) isomers easily. The nuclear magnetic resonance (NMR) spectral technique is a standard and universal approach for structural elucidation (Wang et al., 2018; Song et al., 2019; Li et al., 2020; Wang et al., 2020). In this study, UPLC-Q-TOF-MS/MS analysis combined with purification and NMR spectral experiments was used to characterize AFB_1-degraded products under UV irradiation. The possible photocatalytic mechanism was elucidated, and toxicities of AFB_1 and degraded products (**1**–**7**) were evaluated, which provided a thought for other mycotoxin degradation processes.

EXPERIMENTAL

Chemicals and Reagents

Aflatoxin B_1 was purchased from Pribolab (Qingdao, China). Chromatographic-grade methanol and acetone were obtained from Tianjin Saifu Rui Technology Company (Tianjin, China). Analytical-grade methanol, acetone, and DMSO were obtained from Chron Chemicals (Chengdu, China). For NMR analysis, all deuterium reagents were purchased from Sigma (St. Louis, MO, USA).

Standard solutions of AFB_1 were placed in a 2-ml sealed centrifugal tube, prepared in methanol–DMSO (9:1 v/v), and fully dissolved in methanol using an ultrasound device from Beijing Tianlin Hengtai Technology Company (Beijing, China), and then, it was submitted to be degraded.

UV Irradiation

To investigate the degradation of AFB_1, a UV lamp (20 W, 72 μws/cm^2, GGZ250-1, Shanghai Jiming Special Lighting Appliance Factory) at 365 nm wavelength was used to perform the irradiation experiments. 18 mg of pure AFB_1 was added to acetone solvent, and 10 mg of pure AFB_1 was added to methanol solvent, and both of them were placed in a sealed centrifugal tube and illuminated at room temperature for 45 h (Liu et al., 2010).

HPLC Operation

The degraded products were analyzed and isolated by semipreparative HPLC on SEP LC-52 with an MWD UV detector (Separation (Beijing) Technology Co. Ltd., Beijing, China) using a 250 mm × 10 mm i. d., 5 μm, ODS-A column (YMC, Kyoto, Japan). The mixture in methanol was purified by semipreparative HPLC (55–60% CH_3OH in H_2O, v/v, 2 ml/min, 30 min) and yielded **4** (0.6 mg, t_R = 18.6 min), **3** (0.5 mg, t_R = 22.3 min), **1** (0.5 mg, t_R = 23.8 min), and **2** (0.4 mg, t_R = 27.0 min), respectively. The mixture in acetone was isolated by semipreparative HPLC (40% CH_3OH in H_2O, v/v, 2 ml/min, 3 min; 40–100% CH_3OH in H_2O, v/v, 2 ml/min, 20 min) and yielded **5**, **6** (7.0 mg, t_R = 18.7 min), and **7** (1.5 mg, t_R = 21.2 min).

Determination of Degraded Products

The degraded products were identified by NMR experiments. Compounds were analyzed by UPLC-Q-TOF-MS/MS in positive ion mode. 1D and 2D-NMR spectra were acquired using solvent signals (CD_3OD: δ_H 3.31/δ_C 49.9; C_3D_6O: δ_H 2.05/δ_C 49.9; Pyridine-d_5: δ_H 8.74, 7.58, 7.22/δ_C 150.4, 135.9, and 123.9) on a Bruker 600 spectrometer (^{1}H: 600 MHz) and a Bruker Avance III 500 spectrometer (^{1}H: 500 MHz; ^{13}C: 125 MHz) (Bruker, Rheinstetten, Germany).

UPLC-Q-TOF MS Analysis

AFB_1 and degraded products were analyzed using a UPLC-Q-TOF-MS/MS system (Waters, United States). Chromatographic analysis was carried out with a Waters Acquity UPLC-PDA system equipped with an analytical reverse-phase C-18 column (2.1 × 100 mm, 1.7 μm, Acquity BEH, Waters, United States) with an absorbance range of 200–400 nm. The column temperature was maintained at 40°C. 0.1% formic acid in water (A) and 0.1% formic acid in acetonitrile (B) were used as the mobile phase. The gradient conditions were as follows: 0–10 min, 10 %–60% B; 10–12.5 min, 60 %–95% B; and 12.6–15 min, 10% B. The flow rate from the UPLC system into the ESI-Q-TOF-MS detector was 0.3 ml/min. The auto-injected volume was 3 μl. Time-of-flight MS detection was performed with a Waters SYNAPT G2 HDMS (Waters Corp., Manchester, United Kingdom) TOF mass

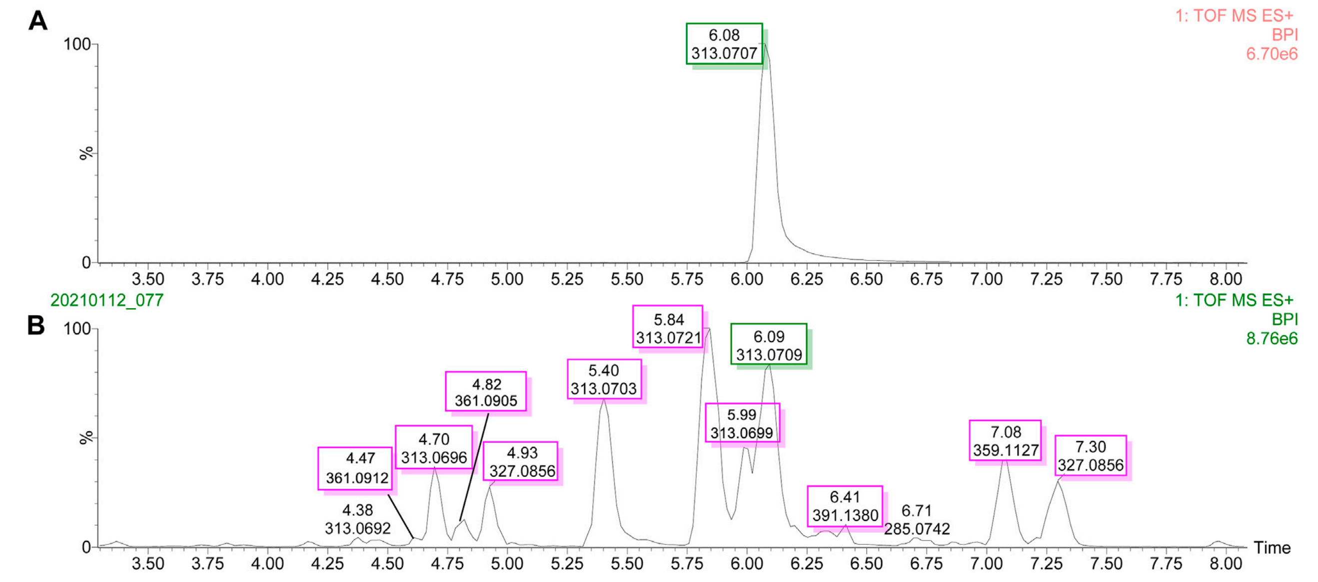

FIGURE 1 | UPLC-Q-TOF-MS/MS profiles of the degradation products of aflatoxin B_1 in methanol solvent. **(A)** Base peak intensity (BPI) of aflatoxin B_1. **(B)** Base peak intensity (BPI) of degradation products of aflatoxin B_1.

spectrometer combined with an ESI source in the positive ion scan mode. The desolvation temperature was set at 400°C with desolvation gas flow at 600 L/h, and the source temperature was 100°C. The lock mass in all analyses was leucine–enkephalin ($[M + H]^+$ = 556.2771), used at a concentration of 0.5 g/ml and infused at a flow rate of 10 L/min. Raw data were acquired using the centroid mode, and the mass range was set from *m/z* 50 to 1200. The capillary voltage was set at 3.0 kV with 40 and 4.0 V of the sample and extraction cone voltage. The collision energy was set as 20 eV for low-energy scan and a ramp from 20 to 30 eV for high-energy scan. The instrument was controlled by MassLynx 4.1 software.

Toxic Evaluation of Degraded Products and AFB_1

All the degraded products and AFB_1 were tested for their cytotoxicity against human normal hepatocytes LO-2 and cancer cell lines Hep-G2 and MCF-7. Cells were incubated in a DMEM high glucose medium (Gibco, USA), added with 10% fetal bovine serum (Gibco, United States) and cultured in a 5% CO_2 incubator at 37°C. The cytotoxicity tests were performed using the MTS (Promega, United States) (Ahmed et al., 2019).

RESULTS AND DISCUSSION

UPLC-Q-TOF-MS/MS Base Peak Intensity and the UPLC Chromatogram of Degraded Products

The UPLC-Q-TOF-MS/MS BPI of AFB_1 and its degraded products in methanol–H_2O and acetone–H_2O solvents are shown in **Figures 1** and **2**. The retention time and molecular weight of AFB_1 were 6.09 min and *m/z* 313 ([M+1]), respectively. A series of degraded products with different retention times (RTs) and molecular weights are shown in **Table 1**. Some ion peaks as (stereo) isomers possessed the same molecular weights (such as *m/z* 345) but with different RTs.

Structural Analysis of Degraded Products Based on Exact Molecular Weights and Fragment Ions

Different free radicals such as reactive hydroxyl ($OH^•$), hydrated electrons ($eaq^−$), hydrogen atoms ($H^•$), and methoxy species ($OCH_3{}^•$) were produced when methanol–H_2O and acetone–H_2O solvents were irradiated under UV (White, 2001; Azrague et al., 2005). These free radicals could attack the AFB_1 structure to form different degraded products. The double bond C_8-C_9 in AFB_1 was broken easily by these free radicals *via* addition reactions. Ten and seven main degraded products in methanol–H_2O and acetone–H_2O solvents were characterized based on molecular weights and fragment ions of compounds (**Supplementary Tables S1, S2**). The other degraded product fragmentation rules are provided in supporting information, considering a similar fragmentation pathway with AFB_1 (**Figure 3** and **Supplementary Figures S2–S9**).

Four ions as (stereo) isomers (*m/z* 345, $C_{18}H_{16}O_7$) appeared at t_R = 4.70, 5.40, 5.84 and 5.99 min in methanol–H_2O solvent with 32 Da (CH_4O) more than that of AFB_1 (**Supplementary Figure S2**). After a neutral loss of CH_3OH from ion (*m/z* 345), the fragmentation pathways of these four ions were nearly the same as those of AFB_1. It is suggested that these four degraded compounds might be addition products of CH_3OH with AFB_1

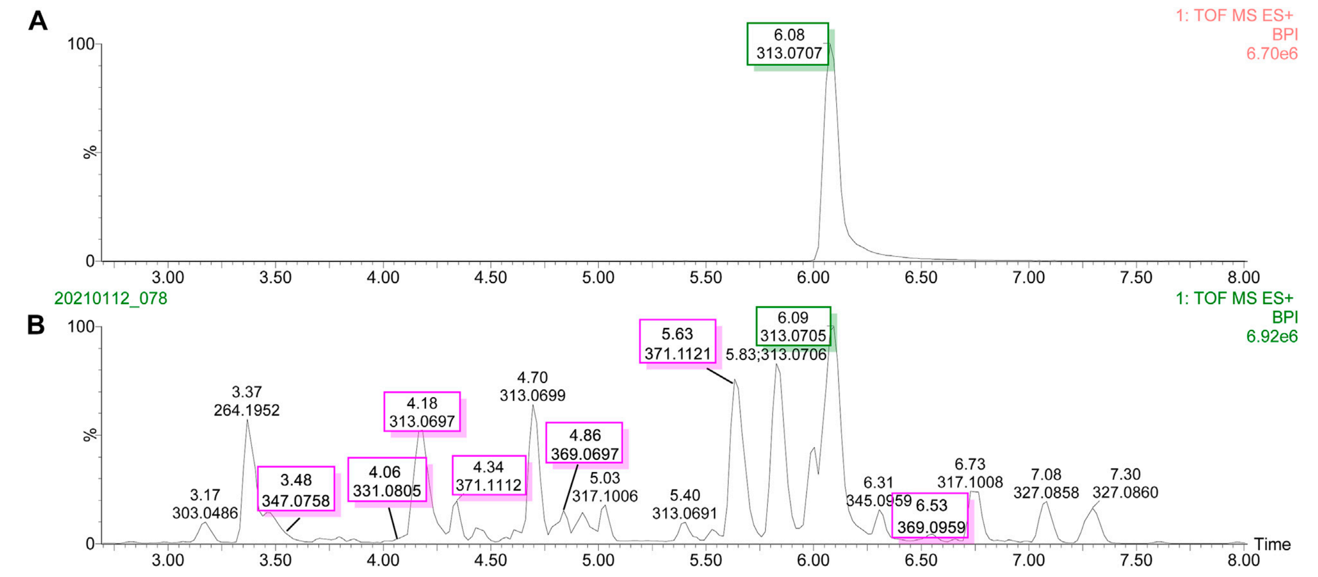

FIGURE 2 | UPLC-Q-TOF-MS/MS profiles of the degradation products of aflatoxin B_1 in acetone solvent. **(A)** Base peak intensity (BPI) of aflatoxin B_1. **(B)** Base peak intensity (BPI) of degradation products of aflatoxin B_1.

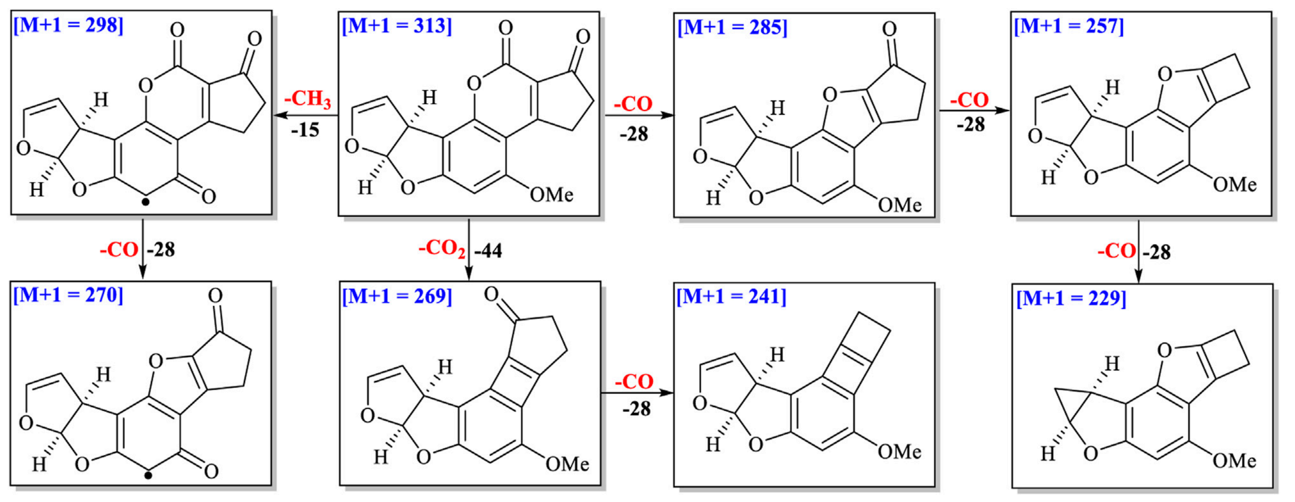

FIGURE 3 | Fragmentation pathway of AFB_1.

at C-8/C-9. The possible fragmentation pathways of these four (stereo) isomers are depicted in **Supplementary Figure S2**.

The molecular formula of the ion at *m/z* 361 ([M+1], t_R = 4.47 and 4.82 min) was determined to be $C_{18}H_{16}O_8$ based on HR-ESI-MS with 16 Da (O) more than that of degraded products (*m/z* 345) (**Supplementary Figure S3**), suggesting one more oxygen atom connected on C_8 or C_9. Both of them were suggested to be the addition products from free radical hydrogen atoms ($OH^•$) and methoxy species ($OCH_3^•$) with C_8/C_9 or C_9/C_8 of AFB_1 under UV irradiation. The possible fragmentation pathway of the ion (*m/z* 361) is shown in **Supplementary Figure S3**.

Three ions at *m/z* 359 ([M+1], t_R = 4.94, 7.08 and 7.30 min) gave the molecular formula as $C_{19}H_{18}O_7$ based on HR-ESI-MS. The neutral loss of -CO, -CH_3OH, and -C_2H_2 was observed in the MS/MS profiles (**Supplementary Figure S4**). The possible structure and fragmentation pathway of these three ions is suggested in **Supplementary Figure S4**.

The molecular formula of the degraded product at *m/z* 391 ([M+1], t_R = 6.41 min) was determined to be $C_{20}H_{22}O_8$ based on HR-ESI-MS (**Supplementary Figure S5**). Sequential losses of two -CH_3OH (391→359→327), one -CH_2O (327→297), and one -CH_2 (297→283) implied that four methoxyls might be present in degraded products. Two methoxyls might be

TABLE 1 | HR-ESI and MS/MS data of seventeen degraded products and aflatoxin B_1.

Structure	Retention time (min)	Extract Mass (m/z)	Formula	Diff (ppm)	Loss mass	Loss formula
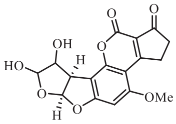	3.48	347.0758	$C_{17}H_{15}O_8$	–2.6		
		329.0648	$C_{17}H_{13}O_7$	–4.0	18.0110	$[M + H]^+$-H_2O
		319.0811	$C_{16}H_{15}O_7$	–2.2	27.9947	$[M + H]^+$-CO
		311.0538	$C_{17}H_{11}O_6$	–5.8	36.0220	$[M + H]^+$-H_2O-H_2O
		301.0697	$C_{16}H_{13}O_6$	–5.0	46.0062	$[M + H]^+$-CO-H_2O
		283.0595	$C_{16}H_{11}O_5$	–3.9	64.0163	$[M + H]^+$-H_2O-H_2O-CO
		273.0747	$C_{15}H_{13}O_5$	–5.9	74.0008	$[M + H]^+$-CO-H_2O-CO
		271.0595	$C_{15}H_{11}O_5$	–4.1	76.0163	$[M + H]^+$-CO-H_2O-HCHO
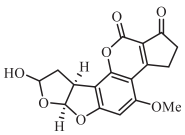	4.06	331.0801	$C_{17}H_{15}O_7$	–5.4		
	4.18	313.0697	$C_{17}H_{13}O_6$	–4.8	18.0104	$[M + H]^+$-H_2O
		301.0699	$C_{16}H_{13}O_6$	–4.3	30.0102	$[M + H]^+$-HCHO
		285.0746	$C_{16}H_{13}O_5$	–6.0	46.0055	$[M + H]^+$-H_2O-CO
		283.0598	$C_{16}H_{11}O_5$	–2.8	48.0203	$[M + H]^+$-CH_2O-H_2O
		273.0378	$C_{14}H_9O_6$	–7.7	58.0423	$[M + H]^+$- CH_2O-CO
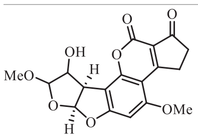	4.47	361.0905	$C_{18}H_{17}O_8$	–5.0		
	4.82	343.0799	$C_{18}H_{15}O_7$	–5.5	18.0106	$[M + H]^+$-H_2O
		329.0643	$C_{17}H_{13}O_7$	–5.5	32.0262	$[M + H]^+$-CH_3OH
		315.0858	$C_{17}H_{15}O_6$	–3.5	46.0047	$[M + H]^+$-H_2O-CO
		311.0542	$C_{17}H_{11}O_6$	–4.5	50.0363	$[M + H]^+$-H_2O-CH_3OH
		301.0698	$C_{16}H_{13}O_6$	–4.7	60.0207	$[M + H]^+$-CH_3OH-CO
		283.0588	$C_{16}H_{11}O_5$	–6.4	78.0317	$[M + H]^+$-CH_3OH-CO-H_2O
		273.0753	$C_{15}H_{13}O_5$	–3.7	88.0152	$[M + H]^+$-CH_3OH-CO-CO
		255.0646	$C_{15}H_{11}O_4$	–4.3	106.0259	$[M + H]^+$-CH_3OH-CO-H_2O-CO
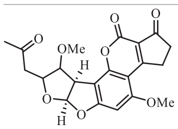	4.86	401.1224	$C_{21}H_{21}O_8$	–3.0		
		369.0967	$C_{20}H_{17}O_7$	–1.9	32.0257	$[M + H]^+$-CH_3OH
		343.0804	$C_{18}H_{15}O_7$	–4.1	58.0420	$[M + H]^+$-CH_3COCH_3
		315.0851	$C_{17}H_{15}O_6$	–5.7	86.0373	$[M + H]^+$-CH_3COCH_3-CO
		313.0697	$C_{17}H_{13}O_6$	–4.8	88.0527	$[M + H]^+$-CH_3COCH_3-CH_2O
	6.53					$[M + H]^+$-CH_3OH-C_3H_4O
		287.0538	$C_{15}H_{11}O_6$	–6.3	114.0686	$[M + H]^+$-CH_3COCH_3-CO-CO
		285.0747	$C_{16}H_{13}O_5$	–5.6	116.0477	$[M + H]^+$-CH_3COCH_3-CO-CH_2O
		283.0601	$C_{16}H_{11}O_5$	–1.8	118.0623	$[M + H]^+$-CH_3COCH_3-CH_2O-CH_2O
						$[M + H]^+$-CH_3OH-C_3H_4O-CH_2O
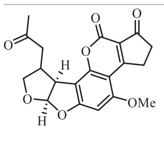	4.345.63	371.1120	$C_{20}H_{19}O_7$	–3.0		
		313.0698	$C_{17}H_{13}O_6$	–4.5	58.0422	$[M + H]^+$-CH_3COCH_3
		285.0751	$C_{16}H_{13}O_5$	–4.2	86.0369	$[M + H]^+$-CH_3COCH_3-CO
		257.0796	$C_{15}H_{13}O_4$	–7.0	114.0324	$[M + H]^+$-CH_3COCH_3-CO-CO
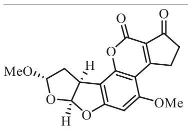	4.70	345.0971	$C_{18}H_{17}O_7$	–0.9		
	5.40	313.0721	$C_{17}H_{13}O_6$	2.0	32.0250	$[M + H]^+$-CH_3OH
	5.84	285.0751	$C_{16}H_{13}O_5$	–4.2	60.0220	$[M + H]^+$-CH_3OH-CO
	5.99	269.0802	$C_{16}H_{13}O_4$	–4.5	76.0169	$[M + H]^+$-CH_3OH-CO_2
		257.0794	$C_{15}H_{13}O_4$	–7.8	88.0171	$[M + H]^+$-CH_3OH-CO-CO
		243.0647	$C_{14}H_{11}O_4$	–4.1	102.0324	$[M + H]^+$-CH_3OH-CO-CO-CH_2
		241.0846	$C_{15}H_{13}O_3$	–7.9	104.0125	$[M + H]^+$-CH_3OH-CO_2-CO
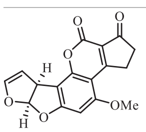	6.09	313.0705	$C_{17}H_{13}O_6$	–2.2	27.9955	$[M + H]^+$-CO
	AFB_1	285.0750	$C_{16}H_{13}O_5$	–4.6	43.9900	$[M + H]^+$-CO_2
		269.0805	$C_{16}H_{13}O_4$	–3.3	55.9912	$[M + H]^+$-CO-CO
		257.0793	$C_{15}H_{13}O_4$	–8.2	72.0211	$[M + H]^+$-CO_2-CO
		241.0494	$C_{14}H_9O_4$	–2.9	83.9857	$[M + H]^+$-CO-CO-CO
		229.0848	$C_{14}H_{13}O_3$	–1.7		
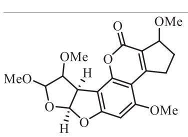	6.41	391.1380	$C_{20}H_{23}O_8$	–3.3		
		359.1111	$C_{19}H_{19}O_7$	–5.6	32.0269	$[M + H]^+$-CH_3OH
		345.0955	$C_{18}H_{17}O_7$	–5.5	46.0425	$[M + H]^+$-CH_3OH-CH_2
		327.0852	$C_{18}H_{15}O_6$	–5.2	64.0528	$[M + H]^+$-CH_3OH-CH_3OH
		313.0696	$C_{17}H_{13}O_6$	–5.1	78.0684	$[M + H]^+$-CH_3OH-CH_2-CH_3OH
		297.0749	$C_{17}H_{13}O_5$	–4.7	94.0631	$[M + H]^+$-CH_3OH-CH_3OH-CH_2O

(Continued on following page)

TABLE 1 | (*Continued*) HR-ESI and MS/MS data of seventeen degraded products and aflatoxin B_1.

Structure	Retention time (min)	Extract Mass (m/z)	Formula	Diff (ppm)	Loss mass	Loss formula
		285.0754	$C_{16}H_{13}O_5$	−3.2	106.0626	$[M + H]^+$-CH_3OH-CH_2-CH_3OH-CO
		283.0597	$C_{16}H_{11}O_5$	−3.2	108.0783	$[M + H]^+$-CH_3OH-CH_3OH-CH_2O-CH_2
		255.0653	$C_{15}H_{11}O_4$	−1.6	136.0727	$[M + H]^+$-CH_3OH-CH_2-CH_3OH-CO
						$[M + H]^+$-CH_3OH-CH_3OH-CH_2O-CH_2-CO
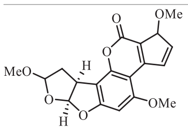	4.93	359.1121	$C_{19}H_{19}O_7$	−2.8		
	7.30	345.0957	$C_{18}H_{17}O_7$	−4.9	14.0164	$[M + H]^+$-CH_2
		327.0856	$C_{18}H_{15}O_6$	−4.0	32.0265	$[M + H]^+$-CH_3OH
		313.0693	$C_{17}H_{13}O_6$	−6.1	46.0428	$[M + H]^+$-CH_2-CH_3OH
		301.0697	$C_{16}H_{13}O_6$	−5.0	58.0424	$[M + H]^+$-CH_3OH-C_2H_2
		299.0904	$C_{17}H_{15}O_5$	−5.0	60.0217	$[M + H]^+$-CH_3OH-CO
		287.0564	$C_{15}H_{11}O_6$	2.8	72.0557	$[M + H]^+$-CH_3OH-C_2H_2-CH_2
		273.0746	$C_{15}H_{13}O_5$	−6.2	86.0375	$[M + H]^+$-CH_3OH-C_2H_2-CO
		259.0594	$C_{14}H_{11}O_5$	−4.6	100.0527	$[M + H]^+$-CH_3COCH_3-CO-CO

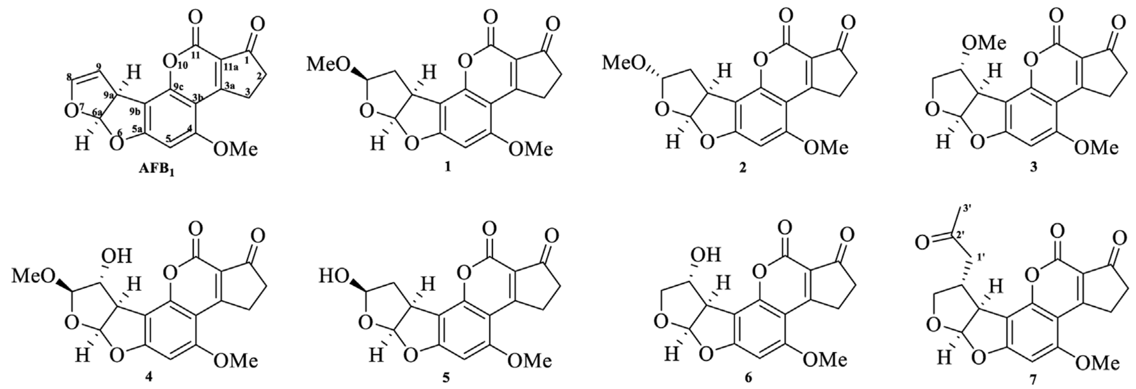

FIGURE 4 | Structures of AFB_1 and 1-7

connected on C-8/C-9 and the keto-carboxyl group might be transformed to another methoxyl through reduction and addition reactions, and the remaining -OMe was anchored on the aromatic ring. The possible fragmentation pathway of these three ions is suggested in **Supplementary Figure S5**.

The molecular formula of ions at *m/z* 331 ([M+1, $C_{17}H_{14}O_7$] in acetone–H_2O at 4.06 and 4.18 min) possessed 18 Da (H_2O) more than that of AFB_1, which indicated these two degraded products were (stereo) isomers (**Supplementary Figure S6**). The fragmentation pathways of these two ions were nearly the same as those of AFB_1 after the loss of a molecule of H_2O, which implied that two degraded products were the adducts of H_2O with the double bond C-8/C-9. Though the molecular formulas and fragmentation pathways of these two degraded products were the same, the retention time and abundance of fragment ions were different. A higher abundance of ion at *m/z* 313 (t_R = 4.18 min) was observed than the other (t_R = 4.06 min). This suggested that the position of OH on the furan ring was different in two degraded products. The possible fragmentation pathway of two ions is suggested in **Supplementary Figure S6**.

The molecular formula of the ion at *m/z* 347 ([M+1], t_R = 3.48 min) was determined to be $C_{18}H_{14}O_8$ based on HR-ESI-MS with 16 Da (O) more than that of degraded products (*m/z* 331), indicating two hydroxyl groups connected on C_8 and C_9, respectively (**Supplementary Figure S7**). The possible fragmentation pathway is suggested in **Supplementary Figure S7**.

The molecular formula of the ion at *m/z* 371 ([M+1], t_R = 4.34 and 5.63 min) was determined to be $C_{20}H_{18}O_7$ based on HR-ESI-MS with 58 Da (CH_3COCH_3) more than that of AFB_1 (*m/z* 313) (**Supplementary Figure S8**), which implied that one molecule of acetone attacked on C-8 or C-9 under UV irradiation. The possible fragmentation pathway of them is suggested in **Supplementary Figure S8**.

The molecular formulas of ions at *m/z* 401 ([M+1], t_R = 4.86 and 6.54 min) were determined to be $C_{21}H_{20}O_8$ based on HR-ESI-MS. The loss of 32 Da from *m/z* 401 to *m/z* 369 and the loss of 58 Da from *m/z* 401 to *m/z* 343 suggested that a methoxyl and acetone were connected on C-8/C-9 or C-9/C-8 (**Supplementary Figure S9**). The possible fragmentation pathway of these two ions is suggested in **Supplementary Figure S9**.

Though seventeen degraded products were characterized by molecular formula and fragment ions, the planar structures and configurations of some degraded products could not be

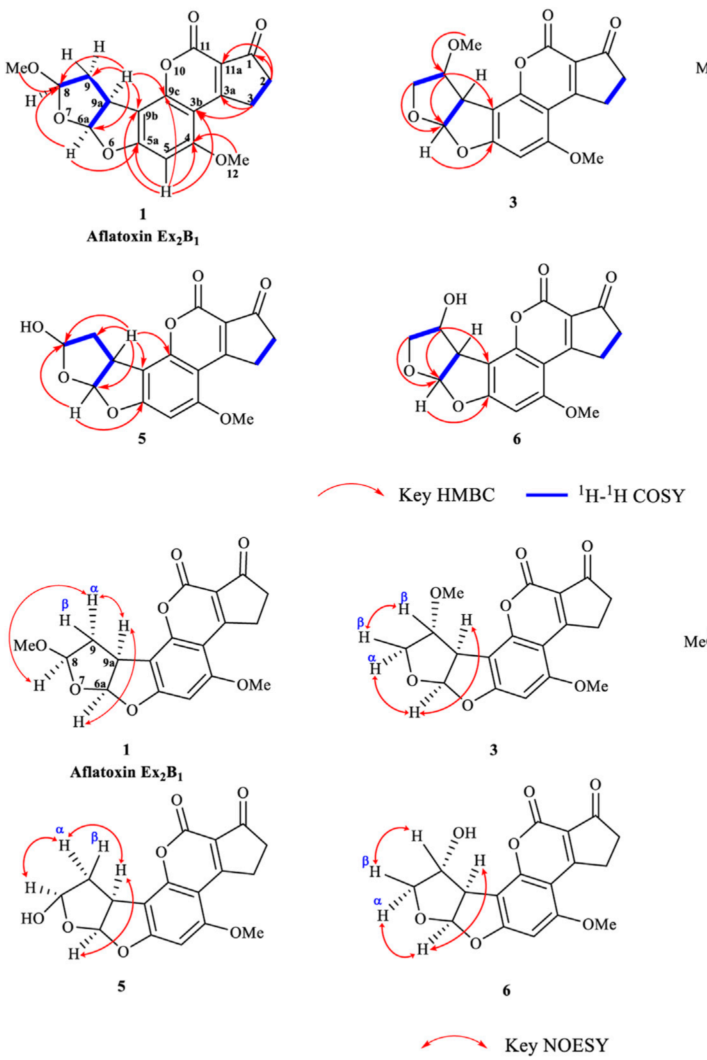

FIGURE 5 | Key 2D-NMR and NOESY correlations of 1 and 3-7

TABLE 2 | ^1H NMR data of compounds **1**-**4** in acetone-d_6 at 600 MHz and **5**-**7** in pyridine-d_5 at 500 MHz.

Pos	1	2	3	4	5	6	7
	δ_H (*J* in Hz)	δ_H (*J* in Hz)	δ_H (*J* in Hz)	δ_H (*J* in Hz)	δ_H (*J* in Hz)	δ_H (*J* in Hz)	δ_H (*J* in Hz)
2	2.51, t (5.4)	2.48, m	2.48, m	2.47, dd (6.0, 4.8)	2.53, ddd (7.0, 4.5, 2.5)	2.57, t (5.5)	2.57, dt (6.5, 5.0)
3	3.42, dt (5.4, 4.2)	3.38, m	3.38, m	3.38, ddd (5.4, 4.2, 3.0)	3.03, m	3.14, m	3.13, m
5	6.54, s	6.54, s	6.52, s	6.50, s	6.54, s	6.59, s	6.56, s
6a	6.60, d (6.0)	6.48, d (6.0)	6.57, d (5.4)	6.65, d (6.0)	6.79, d (6.0)	6.95, d (5.5)	6.74, d (5.5)
8	5.27, d (4.8)	5.15, t (4.8)	4.10, dd (10.8, 1.2)	5.02, s	6.06, d (5.0)	4.44, d (10.0)	4.04, m
			3.66, dd (10.8, 3.0)			4.06, dd (10.0, 3.0)	
9	2.42, ddd (13.2, 9.6, 4.8)	2.31, m	4.12, d (3.0)	4.37, d (3.6)	2.68, d (13.0)	5.02, d (3.0)	3.13, m
	2.27, d (13.2)	2.23, m			2.36, m		
9a	4.19, dd (9.6, 6.0)	4.24, t (6.0)	4.15, d (5.4)	3.95, d (6.0)	4.20, dd (9.5, 6.0)	4.37, d (5.5)	3.93, dd (5.5, 1.0)
4-OCH_3	4.03, s	4.01, s	4.00, s	3.99, s	3.72, s	3.84, s	3.84, s
8-OCH_3	3.16, s	3.37, s		3.11, s			
9-OCH_3			3.43, s				
1′							2.72, d (7.5)
3′							2.12, s

TABLE 3 | ^{13}C NMR data of compounds **1**, **3**, **4** in acetone-d_6 and **5**-**7** in pyridine-d_5 at 125 MHz.

Pos	1	3	4	5	6	7
1	200.9, C	200.8, C	200.8, C	200.8, C	200.8, C	200.8, C
2	35.5, CH_2	35.5, CH_2	35.5, CH_2	35.8, CH_2	35.8, CH_2	36.0, CH_2
3	29.5, CH_2	29.6, CH_2	29.8, CH_2	29.5, CH_2	29.6, CH_2	29.1, CH_2
3a	178.1, C	177.9, C	178.1, C	177.7, C	177.7, C	178.3, C
3b	103.8, C	104.2, C	104.1, C	104.4, C	104.3, C	103.2, C
4	162.7, C	163.0, C	162.9, C	162.4, C	162.6, C	163.1, C
5	91.2, CH	91.0, CH	91.2, CH	92.2, CH	90.7, CH	90.3, C
5a	167.0, C	167.8, C	167.0, C	167.6, C	168.6, C	167.4, C
6a	115.0, CH	114.7, CH	115.0, CH	115.4, CH	115.0, CH	114.3, C
8	107.6, CH	72.6, CH_2	112.5, CH	101.7, CH	76.9, CH_2	73.3, CH_2
9	37.8, CH_2	84.7, CH	78.2, CH	38.9, CH_2	74.7, CH	41.1, CH
9a	43.1, CH	50.7, CH	52.8, CH	43.4, CH	55.2, CH	50.3, CH
9b	109.8, C	107.6, C	106.3, C	110.1, C	105.1, C	107.2, C
9c	153.5, C	154.5, C	153.8, C	154.5, C	154.5, C	154.2, C
11	155.3, C	156.0, C	154.8, C	155.6, C	155.6, C	156.5, C
11a	117.8, C	117.0, C	117.5, C	117.5, C	117.8, C	117.7, C
1′						47.5, CH_2
2′						206.5, C
3′						30.4, CH_3
4-OCH_3	56.9, CH_3	57.1, CH_3	57.1, CH_3	56.7, CH_3	57.8, CH_3	56.8, CH_3
8-OCH_3	55.0, CH_3		54.8, CH_3			
9-OCH_3		56.8, CH_3				

determined only based on UPLC-Q-TOF-MS/MS analysis. Thus, further purification and NMR experiments are needed to elucidate their structures and stereochemistry.

Purification and Elucidation of Seven Degraded Products Structures

Seven main degraded products with limited amounts were purified by HPLC and then elucidated by NMR spectra (**Figure 4**). Compounds 1–3 were isolated as the photochemical adducts of 6-methoxydifurocoumarone, which were analyzed based on the ^{1}H-NMR spectrum (Waiss and Wiley, 1969). In this study, the structures of these three degraded products were elucidated in detail by analyzing ^{1}H, ^{13}C, and 2D-NMR spectra (**Figure 5**). The ^{1}H-NMR data of 1–3 and ^{13}C-NMR data of 1 and 3 are shown in **Table 2** and **Table 3**. The relative configurations of 1 and 3 were determined by NOESY correlations (**Figure 5**). Compound 4 was a new degraded product isolated from methanol solution. The molecular formula of 4 was determined to be $C_{18}H_{17}O_8$ on the basis of HR-ESI-MS with 16 more daltons than that of 1, implying that an additional hydroxyl group was present in 4, which was supported by the NMR spectra (**Table 2** and **Table 3**). The ^{1}H–^{1}H COSY and HMBC correlations confirmed that the additional hydroxyl group was connected on C-9 (**Figure 5**). The NOESY correlations determined the relative configuration of 8-OMe and 9-OH to be β and α configuration, respectively (**Figure 5**).

Compounds 5 and 6 were obtained as an inseparable mixture through HPLC with various stationary and mobile phases, whereas well-resolved NMR spectra determined the structures of 5 and 6 as isomers. The ^{1}H and ^{13}C spectra data of 5 were reported, and 6 was a new degraded product reported for the first time (Cox and Cole, 1977; Liu, Jin, Tao, Shan, et al., 2010; Wang et al., 2011; Wang et al., 2012; Stanley et al., 2020). The molecular formula of 5 and 6 was determined to be $C_{17}H_{14}O_7$ on the basis of HR-ESI-MS, with 18 more daltons than that of AFB_1, implying that 5 and 6 might be transformed from AFB_1 through an addition reaction with H_2O on the double bond (C-8/C-9). The planar and relative configurations of 5 and 6 were established based on 2D-NMR data (**Figure 5**). Compound 7 was a new degraded product isolated from acetone solvent. The molecular formula of 7 was established to be $C_{20}H_{19}O_7$ based on HR-ESI-MS. In the ^{1}H NMR spectrum, an additional methyl (δ_H = 2.12 ppm) and an additional methylene unit (δ_H = 2.72 ppm) were observed compared with that of AFB_1, which indicated that one molecule of acetone might be connected on C-8 or C-9. The ^{1}H–^{1}H COSY and HMBC correlations confirmed that the acetonyl group was connected with C-9 (**Figure 5**). The NOESY correlations from H-9a (δ_H = 3.93 ppm) to H-1' (δ_H = 2.72 ppm) determined the acetonyl group to be α-configuration (**Figure 5**). Considering that the stereochemistry of C-6a and C-9a were not changed in the photocatalytic reaction, the absolute configurations of (**1**–**7**) are shown in **Figure 4**.

Elucidation of the Photodegraded Mechanism of Degraded Products

According to the structural features of AFB_1 and degraded products (1–7), the possible photocatalytic reactions were suggested: 1) addition reactions happened between MeOH, H_2O, or acetone with AFB_1 under UV irradiation to produce compounds such as 1–3 and 5–7; 2) compound 4 might be originated from the oxygen free radical attacking the double bond (C-8/C-9) to form an epoxide, which was further attacked by $OMe^\bullet$ or $OH^\bullet$ (**Figure 6**) (Waiss and Wiley, 1969; Iyer et al., 1994). The photocatalytic mechanism was suggested: MeOH, H_2O, or CH_3COCH_3 formed potential free radicals ($H^\bullet$, $OH^\bullet$, $OMe^\bullet$, or $CH_3COCH_2^\bullet$) under UV irradiation. Then, $H^\bullet$ attacked on the double bond (C-8 or C-9) leading to form carbon-free radicals, which was then coupled with $OH^\bullet$, $OMe^\bullet$, or $CH_3COCH_2^\bullet$ to shape degraded products 1–3 and 5–7 (Waiss and

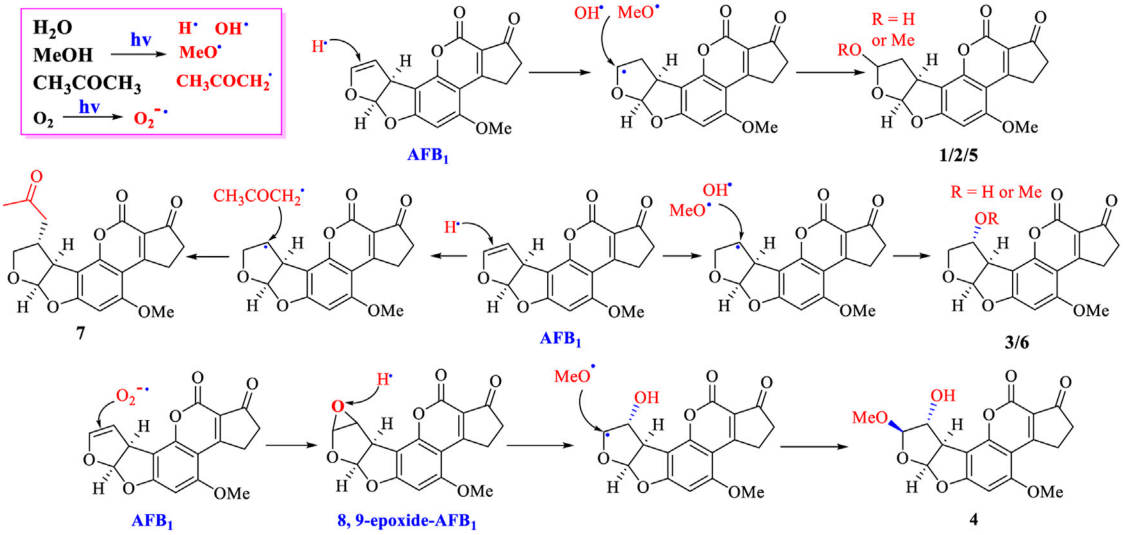

FIGURE 6 | Possibly photocatalytic mechanism of AFB$_1$ in MeOH and acetone.

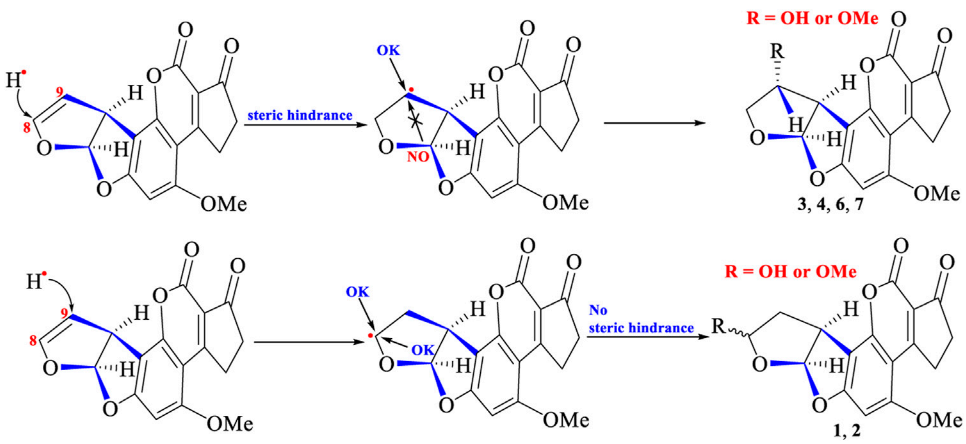

FIGURE 7 | Possible catalytic reaction happened at C-8 and C-9

TABLE 4 | Cytotoxic activity of seven degraded products and aflatoxin B$_1$.

Compounds	Cytotoxic activity (μM)		
	LO-2	Hep-G2	MCF-7
AFB$_1$	22.47 ± 3.10	29.08 ± 4.92	36.57 ± 4.43
1	>100	>100	>100
2	>100	>100	>100
3	>100	>100	>100
4	>100	>100	>100
5/6	>100	>100	>100
7	>100	>100	>100
cis-platinum	6.54 ± 0.72	11.36 ± 1.47	21.47 ± 2.18

Wiley, 1969; Iyer et al., 1994; Jamil et al., 2017; Mao et al., 2019). In addition, O_2 in the air under UV irradiation could form $O_2^{\bullet -}$, which could attack on the double bond C-8/C-9 to produce 8,9-epoxide-AFB$_1$. Addition reactions then happened fast by the highly unstable intermediate 8,9-epoxide-AFB$_1$ with OMe$^\bullet$ to form the degraded products of 4 (**Figure 6**) (Waiss and Wiley, 1969; Iyer et al., 1994; Jamil et al., 2017).

From the structural features of degraded products (1–7), an interesting phenomenon was also observed that the group of C-9 (in 3, 4, 6, and 7) was α-configuration, whereas the group of C-8 in 1 and 2 was α- or β-configuration. This demonstrated that steric hindrance (from right part of AFB$_1$ structure) might exist and prevent different groups (OH$^\bullet$, OMe$^\bullet$, or $CH_3COCH_2^\bullet$) attacking C-9 from the positive face (β-position), whereas C-8 could be attacked from two sides (α- or β-configuration) without steric hindrance. The crystal structure of AFB$_1$ (Cheung and Sim, 1964; van Soest and Peerdeman, 1970) revealed that the right part of the AFB$_1$ structure was indeed closer to C-9 than C-8 in space, which might preclude different groups to attack C-9 from the positive face (β-position) due to spatial hindrance. The photocatalytic reactions are depicted in **Figure 7**.

Toxic Evaluation of Degraded Products

The cytotoxicity of AFB_1 and seven degraded products (1–7) was evaluated against human normal hepatocytes LO-2 and cancer cell lines Hep-G2 and MCF-7 using the MTS method, with *cis*-platinum as the positive control; the results are shown in **Table 4**. AFB_1 displayed stronger cytotoxicity to three cell lines than the degraded products, further supporting that the double bond (C-8/C-9) in the furan ring was the key toxic group, and the toxicity was markedly reduced after the double bond was broken.

CONCLUSION

In this work, the degraded products of AFB_1 under UV irradiation were analyzed through UPLC-Q-TOF-MS/MS, and seventeen degraded products were characterized. Seven degraded products were purified and elucidated by NMR experiments. The double bond (C-8/C-9) of all degraded products was broken, which was coupled with different groups such as $OH^{\bullet}$, $H^{\bullet}$, and $OCH_3^{\bullet}$ through addition reactions under UV irradiation. The cytotoxic evaluation revealed that the toxicity of AFB_1-degraded products was markedly reduced after their double bond in the furan ring was cleaved. The results demonstrated that the UPLC-Q-TOF-MS/MS technique coupled with purification NMR analysis and biological tests was an applicably integrated approach for the analysis, characterization, and toxic evaluation of degraded products of AFB_1, which can also be used to evaluate other mycotoxin degradation processes.

DATA AVAILABILITY STATEMENT

The datasets presented in this study can be found in online repositories. The names of the repository/repositories and accession number(s) can be found in the article/ **Supplementary Material**.

AUTHOR CONTRIBUTIONS

Methodology, Y-DW and C-GS; formal analysis, GD; resources, JY; bioassay, TZ and Y-YZ; writing—original draft preparation, GD; and writing—review and editing, J-CQ and L-PG.

FUNDING

This work was supported by the Key Project at Central Government Level: The Ability Establishment of Sustainable Use for Valuable Chinese Medicine Resources (2060302), the National Natural Science Foundation of China (No. 81891014), the National Key R&D Program of China (No. 2017YFC1700701), and the Fundamental Research Funds for the Central public welfare research institutes (No. ZZXT201906).

SUPPLEMENTARY MATERIAL

The Supplementary Material for this article can be found online at: https://www.frontiersin.org/articles/10.3389/fchem.2021.789249/full#supplementary-material

REFERENCES

Ahmed, M. Y., Salah, M. M., Kassim, S. K., Abdelaal, A., Elayat, W. M., Mohamed, D. A.-W., et al. (2019). Evaluation of the Diagnostic and Therapeutic Roles of Non-Coding RNA and Cell Proliferation Related Gene Association in Hepatocellular Carcinoma. *Gene.* 706, 97–105. doi:10.1016/j.gene.2019.04.054

Alberts, J. F., Gelderblom, W. C. A., Botha, A., and van Zyl, W. H. (2009). Degradation of Aflatoxin B_1 by Fungal Laccase Enzymes. *Int. J. Food Microbiol.* 135, 47–52. doi:10.1016/j.ijfoodmicro.2009.07.022

Azrague, K., Bonnefille, E., Pradines, V., Pimienta, V., Oliveros, E., Maurette, M. T., et al. (2005). Hydrogen Peroxide Evolution during V-UV Photolysis of Water. *Photochem. Photobiol. Sci.* 4, 406–408. doi:10.1039/b500162e

Calado, T., Venâncio, A., and Abrunhosa, L. (2014). Irradiation for Mold and Mycotoxin Control: A Review. *Compr. Rev. Food Sci. Food Saf.* 13, 1049–1061. doi:10.1111/1541-4337.12095

Cancer, I. (1993). Some Naturally Occurring Substances: Food Items and Constituents, Heterocyclic Aromatic Amines and Mycotoxins. *Carcinogenesis.* 56, 245–395.

Cheung, K. K., and Sim, G. A. (1964). Aflatoxin G_1: Direct Determination of the Structure by the Method of Isomorphous Replacement. *Nature.* 201, 1185–1188. doi:10.1038/2011185a0

Colin Garner, R., Miller, E. C., Miller, J. A., Garner, J. V., and Hanson, R. S. (1971). Formation of a Factor Lethal for S. Typhimurium TA1530 and TA1531 on Incubation of Aflatoxin B_1 With Rat Liver Microsomes. *Biochem. Biophysical Res. Commun.* 45, 774–780. doi:10.1016/0006-291x(71)90484-0

Cox, R. H., and Cole, R. J. (1977). Carbon-13 Nuclear Magnetic Resonance Studies of Fungal Metabolites, Aflatoxins, and Sterigmatocystins. *J. Org. Chem.* 42, 112–114. doi:10.1021/jo00421a022

Croy, R. G., Essigmann, J. M., Reinhold, V. N., and Wogan, G. N. (1978). Identification of the Principal Aflatoxin B_1-DNA Adduct Formed *In Vivo* in Rat Liver. *Proc. Natl. Acad. Sci.* 75, 1745–1749. doi:10.1073/pnas.75.4.1745

Essigmann, J. M., Croy, R. G., Nadzan, A. M., Busby, W. F., Reinhold, V. N., Buchi, G., et al. (1977). Structural Identification of the Major DNA Adduct Formed by Aflatoxin B_1 *In Vitro*. *Proc. Natl. Acad. Sci.* 74, 1870–1874. doi:10.1073/pnas.74.5.1870

Iyer, R. S., Coles, B. F., Raney, K. D., Thier, R., Guengerich, F. P., and Harris, T. M. (1994). DNA Adduction by the Potent Carcinogen Aflatoxin B_1: Mechanistic Studies. *J. Am. Chem. Soc.* 116, 1603–1609. doi:10.1021/ja00084a001

Jamil, T. S., Abbas, H. A., Nasr, R. A., El-Kady, A. A., and Ibrahim, M. I. M. (2017). Detoxification of Aflatoxin B_1 Using Nano-Sized Sc-Doped $SrTi_{0.7}$ $Fe_{0.3}$ O3 Under Visible Light. *J. Photochem. Photobiol. A: Chem.* 341, 127–135. doi:10.1016/j.jphotochem.2017.03.023

Kumar, P., Mahato, D. K., Kamle, M., Mohanta, T. K., and Kang, S. G. (2017). Aflatoxins: a Global Concern for Food Safety, Human Health and Their Management. *Front. Microbiol.* 07, 2170. doi:10.3389/fmicb.2016.02170

Li, Y. Y., Tan, X. M., Wang, Y. D., Yang, J., Zhang, Y. G., Sun, B. D., et al. (2020). Bioactive *Seco*-Sativene Sesquiterpenoids from an Artemisia Desertorum Endophytic Fungus, Cochliobolus Sativus. *J. Nat. Prod.* 83, 1488–1494. doi:10.1021/acs.jnatprod.9b01148

Lin, J. K., Miller, J. A., and Miller, E. C. (1977). 2,3-Dihydro-2-(guan-7-yl)-3-hydroxy-aflatoxin B1, a Major Acid Hydrolysis Product of Aflatoxin B1-DNA or -ribosomal RNA Adducts Formed in Hepatic Microsome-Mediated Reactions and in Rat Liver *In Vivo*. *Cancer Res.* 37, 4430–4438.

Liu, R., Jin, Q., Huang, J., Liu, Y., Wang, X., Mao, W., et al. (2011). Photodegradation of Aflatoxin B_1 in Peanut Oil. *Eur. Food Res. Technol.* 232, 843–849. doi:10.1007/s00217-011-1452-6

Liu, R., Jin, Q., Tao, G., Shan, L., Huang, J., Liu, Y., et al. (2010). Photodegradation Kinetics and Byproducts Identification of the Aflatoxin B_1 in Aqueous Medium by Ultra-Performance Liquid Chromatography-Quadrupole Time-Of-Flight Mass Spectrometry. *J. Mass. Spectrom.* 45, 553–559. doi:10.1002/jms.1741

Liu, R., Jin, Q., Tao, G., Shan, L., Liu, Y., and Wang, X. (2010). LC-MS and UPLC-Quadrupole Time-Of-Flight MS for Identification of Photodegradation Products of Aflatoxin B_1. *Chroma.* 71, 107–112. doi:10.1365/s10337-009-1354-y

Luo, X., Wang, R., Wang, L., Li, Y., Zheng, R., Sun, X., et al. (2014). Analyses by UPLC Q-TOF MS of Products of Aflatoxin B1after Ozone Treatment. *Food Additives & Contaminants: A.* 31, 105–110. doi:10.1080/19440049.2013.853323

Mao, J., He, B., Zhang, L., Li, P., Zhang, Q., Ding, X., et al. (2016). A Structure Identification and Toxicity Assessment of the Degradation Products of Aflatoxin B_1 in Peanut Oil under UV Irradiation. *Toxins.* 8, 332. doi:10.3390/toxins8110332

Mao, J., Li, P., Wang, J., Wang, H., Zhang, Q., Zhang, L., et al. (2019). Insights into Photocatalytic Inactivation Mechanism of the Hypertoxic Site in Aflatoxin B_1 over Clew-Like WO3 Decorated with CdS Nanoparticles. *Appl. Catal. B: Environ.* 248, 477–486. doi:10.1016/j.apcatb.2019.01.057

Massey, T. E., Stewart, R. K., Daniels, J. M., and Liu, L. (1995). Biochemical and Molecular Aspects of Mammalian Susceptibility to Aflatoxin B1 Carcinogenicity. *Exp. Biol. Med.* 208, 213–227. doi:10.3181/00379727-208-43852a

Méndez-Albores, A., Veles-Medina, J., Urbina-Álvarez, E., Martínez-Bustos, F., and Moreno-Martínez, E. (2009). Effect of Citric Acid on Aflatoxin Degradation and on Functional and Textural Properties of Extruded Sorghum. *Anim. Feed Sci. Techn.* 150, 316–329. doi:10.1016/j.anifeedsci.2008.10.007

Peng, Z., Chen, L., Zhu, Y., Huang, Y., Hu, X., Wu, Q., et al. (2018). Current Major Degradation Methods for Aflatoxins: a Review. *Trends Food Sci. Techn.* 80, 155–166. doi:10.1016/j.tifs.2018.08.009

Rustom, I. Y. S. (1997). Aflatoxin in Food and Feed: Occurrence, Legislation and Inactivation by Physical Methods. *Food Chem.* 59, 57–67. doi:10.1016/s0308-8146(96)00096-9

Song, B., Li, L.-Y., Shang, H., Liu, Y., Yu, M., Ding, G., et al. (2019). Trematosphones A and B, Two Unique Dimeric Structures from the Desert Plant Endophytic Fungus Trematosphaeria Terricola. *Org. Lett.* 21, 2139–2142. doi:10.1021/acs.orglett.9b00454

Stanley, J., Patras, A., Pendyala, B., Vergne, M. J., and Bansode, R. R. (2020). Performance of a UV-A LED System for Degradation of Aflatoxins B1 and M1 in Pure Water: Kinetics and Cytotoxicity Study. *Sci. Rep.* 10, 13473. doi:10.1038/s41598-020-70370-x

van Soest, T. C., and Peerdeman, A. F. (1970). The crystal Structures of Aflatoxin B1. II. The Structure of an Orthorhombic and a Monoclinic Modification. *Acta Crystallogr. Sect B.* 26, 1947–1955. doi:10.1107/s056774087000523x

Waiss, A. C., and Wiley, M. (1969). Anomalous Photochemical Addition of Methanol to 6-Methoxydifurocoumarone. *J. Chem. Soc. D.* 10, 512–513. doi:10.1039/c29690000512

Wang, F., Xie, F., Xue, X., Wang, Z., Fan, B., and Ha, Y. (2011). Structure Elucidation and Toxicity Analyses of the Radiolytic Products of Aflatoxin B_1 in Methanol-Water Solution. *J. Hazard. Mater.* 192, 1192–1202. doi:10.1016/j.jhazmat.2011.06.027

Wang, H., Lu, Z., Qu, H.-J., Liu, P., Miao, C., Zhu, T., et al. (2012). Antimicrobial Aflatoxins from the marine-derived Fungus Aspergillus flavus 092008. *Arch. Pharm. Res.* 35, 1387–1392. doi:10.1007/s12272-012-0808-1

Wang, M.-H., Hu, Y.-C., Sun, B.-D., Yu, M., Niu, S.-B., Guo, Z., et al. (2018). Highly Photosensitive Poly-Sulfur-Bridged Chetomin Analogues from Chaetomium Cochliodes. *Org. Lett.* 20, 1806–1809. doi:10.1021/acs.orglett.8b00304

Wang, M.-H., Zhang, X.-Y., Tan, X.-M., Niu, S.-B., Sun, B.-D., Yu, M., et al. (2020). Chetocochliodins A-I, Epipoly(Thiodioxopiperazines) from Chaetomium Cochliodes. *J. Nat. Prod.* 83, 805–813. doi:10.1021/acs.jnatprod.9b00239

White (2001). *Determination of Photochemical Production of Hydroxyl Radical by Dissolved Organic Matter and Associated Iron Complexes in Natural Waters.* Ohio State University.

Conflict of Interest: The authors declare that the research was conducted in the absence of any commercial or financial relationships that could be construed as a potential conflict of interest.

Publisher's Note: All claims expressed in this article are solely those of the authors and do not necessarily represent those of their affiliated organizations, or those of the publisher, the editors, and the reviewers. Any product that may be evaluated in this article, or claim that may be made by its manufacturer, is not guaranteed or endorsed by the publisher.